Journal of Applied Fluid Mechanics, Vol. 16, No. 10, pp. 2041-2053, 2023.
Available online at www.jafmonline.net, ISSN 1735-3572, EISSN 1735-3645.
https://doi.org/10.47176/jafm.16.10.1801

CRDI Engine Emission Prediction Models with Injection Parameters Based on ANN and SVM to Improve the SOOT-NOx Trade-Off

W. R. Liao[1], J. H. Shi[2†] and G. X. Li[2]

[1] *College of Mechanical and Electrical Engineering, Changjiang Institute of Technology, Wuhan, Hubei Province, 430212, China*
[2] *College of Mechanical and Vehicle Engineering, Taiyuan University of Technology, Taiyuan, Shanxi Province, 030024, China*

†*Corresponding Author Email: jhshi25@163.com*

ABSTRACT

Artificial Neural Network (ANN) and Support Vector Machine (SVM) have been widely used to solve non-linear problems. In the current study, based on 112 groups of experimental data, ANN and SVM models were established and compared to improve the trade-off relationship between SOOT and NOx emissions of a Common Rail Diesel Injection (CRDI) engine fueled with Fischer-Tropsch (F-T) diesel under different operating conditions and injection parameters. The model parameters for the different predictive targets were selected by evaluating the mean square error (MSE) and determination coefficient. Compared to the number of network iterations, the number of implied nodes had a greater effect on the MSE of the ANN model. Compared to the penalty parameter, the width coefficient had a weaker impact on the SVM performance. A comparative analysis showed that the SVM had better predictive accuracy and generalization ability than the ANN, with a maximum error not exceeding five percent and a determination coefficient of over 0.9. Subsequently, the optimal SVM model was combined with the NSGA-II algorithm to determine the optimal injection parameters for the CRDI engine, resulting in solutions to simultaneously decrease the SOOT and NOx emissions. The optimized injection parameters resulted in a 3.7–7.1% reduction in SOOT emission and a 1.2–2.6% reduction in NOx emissions compared to the original engine operating conditions. Based on limited experimental samples, SVM is inferred to be a useful tool for predicting the exhaust emissions of engines fueled with F-T diesel and can provide support for optimizing injection parameters.

Article History

Received February 1, 2023
Revised May 26, 2023
Accepted June 6, 2023
Available online July 29, 2023

Keywords:

CRDI engine
F-T diesel
Machine learning algorithm
Emission
Model optimization

1. INTRODUCTION

After a long period of market competition and technological development, diesel engines have been widely used in many types of vehicles and equipment owing to their superior dynamic performance, flexible fuel characteristics, and excellent operating reliability, which are heading towards the trends of integration, intelligence, and emission-free. Diesel engines have high dimensionality and strong nonlinearity. Therefore, it is necessary to apply intelligent machine learning algorithms to solve diesel engine problems. The Mobile Source Environmental Management Annual Report (2022) showed that national emissions of nitrogen oxides (NOx) and particulate matter (PM) were 5.821 million tons and 69000 tons, respectively, in 2021. Of these, NOx emissions from diesel vehicles exceeded 80% of the total vehicle emissions, and SOOT emissions exceeded 90%. As diesel vehicles are the main sources of emissions, it is very important to reduce both SOOT and NOx emissions. However, owing to the different mixing formation and combustion processes, there is a trade-off between SOOT and NOx emissions. Many researchers have attempted to improve diesel engine performance with clean alternative fuels and system modeling approaches (Guardiola et al., 2011; Vishwanathan & Reitz, 2015; Zhao et al., 2017; Shi et al., 2018; Şener, 2022).

Fischer-Tropsch (F-T) fuel synthesized from coal is considered one of the most promising alternatives to conventional diesel fuel owing to its excellent fuel properties and ability to improve diesel engine exhaust emissions (Kim et al., 2016; Shi et al., 2019; Neves et al., 2020; Pastor et al., 2020; Soloiu et al., 2020). F-T is similar to diesel fuel with respect to a few physical and chemical characteristics, thus allowing it to be directly used in diesel engines without any modification.

NOMENCLATURE

ANN	Artificial Neural Network	HC	hydrocarbon
BTDC	Before Top Death Center	k	kernel function
C	penalty parameter	MSE	mean square error
CA	crank angle	NOx	nitrogen oxides
CRDI	Common Rail Diesel Injection	NSGA-II	non-dominated sorting genetic algorithm-II
E	output error	PM	particulate matter
ECU	Electronic Control Unit	R^2	determination coefficient
ε	loss function	RBF	Radial Basis Function
F-T	Fischer-Tropsch	SVM	Support Vector Machine
g	width coefficient	WT	Wavelet Threshold

Therefore, research has been conducted on testbed engines powered with F-T diesel to investigate their performance and emissions. Hao et al. (2014) studied a four-cylinder light-duty engine fueled with F-T, and observed a 27.2–44.6% reduction in the total carbonyl exhaust compared to using diesel fuel in the test mode. Jiao et al. (2019) investigated the performance and emission of a diesel engine with diesel and F-T blends at various load conditions. The result indicated that using F-T significantly reduced Particulate matter (PM), while the NOx increased with a small range. It is worth noting that there are also some differences between F-T and commercial diesel in terms of the cetane number, heat value, distillation temperature, and sulfur and aromatic content. The ignition delay is reduced, and the combustion duration is shortened in the F-T combustion phase. However, the injection parameters of diesel engines have not been adjusted or redesigned for new characteristics. Thus, it is impossible to fully utilize and highlight the performance advantages of F–T when engines are operated with the original injection parameters.

In general, bench tests are the most reliable and convincing method. However, these depend exclusively on tests, and have been unable to fulfill the demands of more complex diesel engine systems. Moreover, experiments on diesel engines require considerable time and monetary expenses, which may be unacceptable for research. The emission formation process in modern diesel engines is complex, transient, and non-linear. Accordingly, the application of statistical methods to predict emission performance is inappropriate and lacks accuracy. Artificial intelligence methods, such as artificial neural networks (ANN) and support vector machines (SVM), are promising alternatives for solving such complex and non-linear problems and have become popular for predicting engine performance (Molina et al., 2014). For instance, Aydın et al. (2020) investigated the relationship between engine performance and injection parameters, and developed an engine emission predictive model based on an ANN. The regression coefficient between the emissions and parameters was 0.9858, and the mean relative error was less than 10%. Krishnamoorthi et al. (2019) designed an ANN model using the speed, load, and compression ratio as inputs to optimize the engine emission responses. They found that Hydrocarbon (HC) and NOx emissions decreased by 9.16% and 4.19%, respectively. Some applications of SVM to predict engine performance with various running parameters have been proposed, and the accuracy of such models has been effectively improved (Duan et al., 2018; Emiroğlu & Şen, 2018; Gürgen et al., 2018; Chandran, 2020; Hao et al., 2020). On the other hand, Shamshirband et al. (2016) compared four SVM-based approaches in modeling the energetic parameters of a diesel engine fueled with diesel/biodiesel blends. The results confirmed that the Support Vector Machine-Wavelet Threshold (SVM-WT) approach was the most efficient in energetic modeling. In a similar research, Meenal and Selvakumar (2018) evaluated and compared the accuracy of SVM, ANN and solar radiation models to predict mean solar radiation. The SVM and ANN models have performed better than the solar radiation model for solar applications. SVM and ANN have been widely used in non-linear system modeling because of their unique capabilities in prediction and regression analysis. However, it is challenging and arduous to build an appropriate artificial machine model for a given problem.

In this study, we investigated the relationship between the emission characteristics and injection parameters of a diesel engine fueled with F-T. Therefore, predictive ANN and SVM models based on limited experimental samples were established, and the engine emission characteristics were simulated by varying the operational parameters to achieve the desired objectives of the study. However, it should be noted that the accuracy of ANN models is affected by the selection of neurons and the iteration number, whereas SVM models mainly depend on the kernel function parameters and error penalty factors. Therefore, to improve the accuracy of the predictive model used in this study, the optimal values of the parameters that significantly affect the model performance, were selected. Based on the optimal SVM model, a genetic optimization algorithm was used to determine the optimal injection parameters for diesel engines to simultaneously reduce SOOT and NOx. It is confirmed that the machine self-learning models developed in this study can be utilized to predict and optimize engine performance to achieve minimum emissions.

2. MATERIALS AND METHODS

2.1 CRDI Engine Test System and Procedure

This research was conducted with a CRDI engine fueled with F-T diesel to measure SOOT and NOx emissions under different operating conditions and

Table 1 Main characteristics of F-T diesel and national standard 0# diesel

Parameter	F-T diesel	0# diesel
Initial distillation point (℃)	181	≤180
Final distillation point (℃)	296	≤365
Aromatic content (%)	0.009	≤7.0
Sulfur content ($mg \cdot kg^{-1}$)	0	≤10.0
Low calorific value ($kJ \cdot kg^{-1}$)	42600	44200
Cetane number	62.5	51.0

Table 2 Main specifications of the test engine

Specifications	-
Model	CRDI
Intake type	Charge inter-cooling
Calibration power (kW)	85
Calibration speed (r/min)	3200
Maximum torque (Nm) /speed (r/min)	315/1600–2400
Engine displacement (L)	3.298
Bore × stroke (mm × mm)	100 × 105
Compression ratio	18

injection parameters. The main characteristics of the F-T diesel and national standard 0# diesel are listed in Table 1.

The ET2000 measurement and control system was used to adjust and measure the speed, torque, and other parameters. The primary specifications of the test engine are listed in Table 2.

To ensure the reliability and comparability of the results, the intake air temperature, inlet air pressure, and cooling water temperature were maintained within a certain range throughout the test. Figure 1 shows a schematic of the engine test bench. An open ECU, designed and developed by the Kunming University of Science and Technology, was used to adjust and obtain the injection parameters according to the engine operating conditions. Micro-soot 483 and SESAM I60 developed by AVL List GmbH were used for NOx and SOOT emission collection, respectively. A fuel consumption meter and fuel injection system developed by the Bosch Company were adopted to realize flexible adjustment and calculation of fuel injection. Moreover, to ensure the accuracy of the test data, each operating condition was tested three times, and the average value was used for the analysis.

The study of diesel engine emission predictions belongs to a class of typical non-linear research categories. Many parameters affect the emission performance of diesel engines, such as the engine speed, engine torque, intake temperature, intake pressure, exhaust temperature,

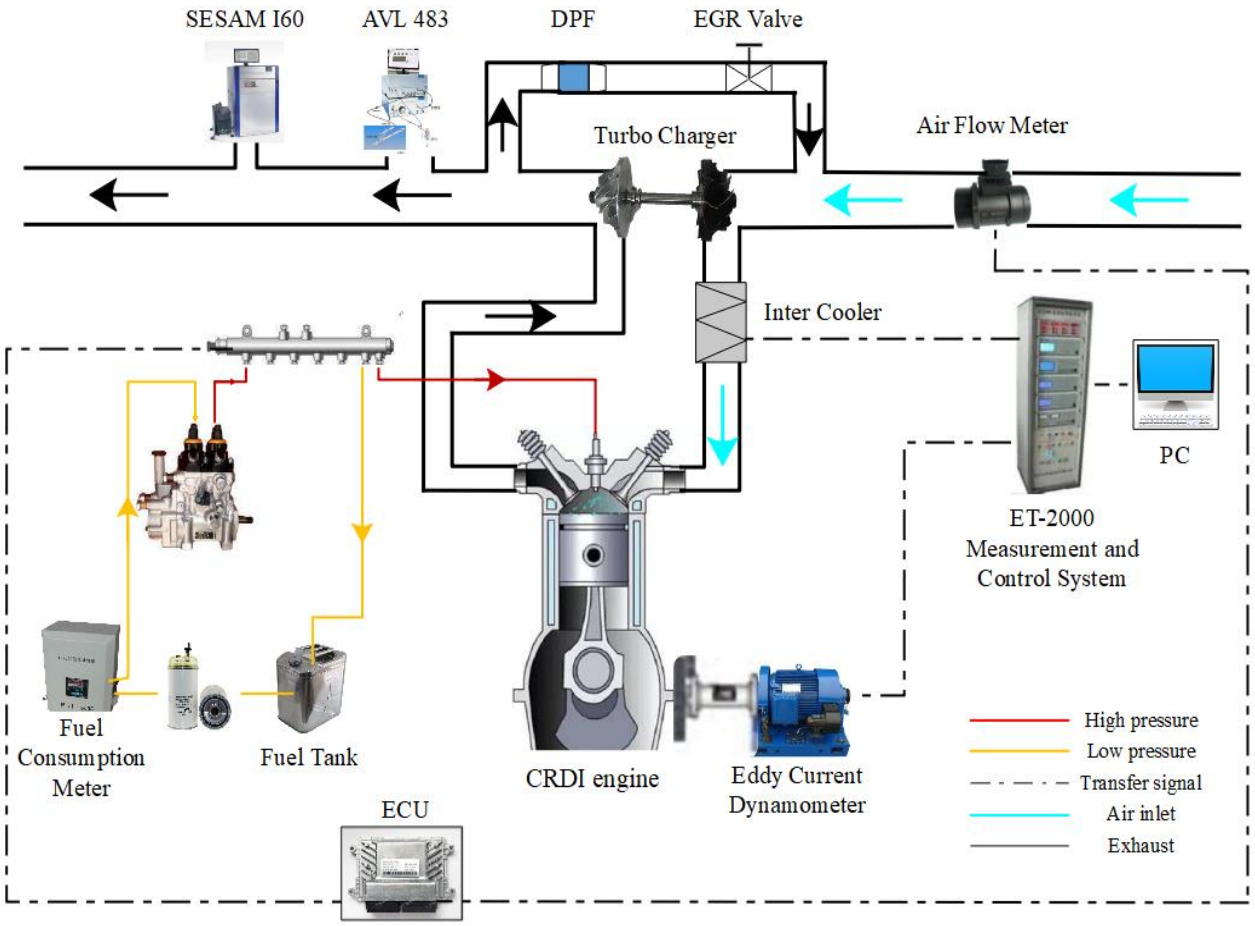

Fig. 1 Schematic diagram of engine test bench

Table 3 Original injection parameters

Speed (r/min)	Torque (Nm)	Pilot injection timing (°CA BTDC)	Main injection timing (°CA BTDC)	Injection pressure (MPa)	Pilot injection quantity (mg/cyc)
1600	50	11.4	4.6	69.0	1.86
	100	13.5	5.4	88.1	2.05
2000	50	12.0	5.2	77.0	1.88
	100	14.0	5.9	95.0	2.08
Adjustment range		±1	±0.5	±5	±0.2

Table 4 Accuracy and uncertainty of the measuring equipment

Instrument	Parameters	Range	Accuracy	Uncertainty (%)
Electric eddy current dynamometer	Speed (r/min)	0–8000	0.10%	-
	Torque (Nm)	0–600	0.40%	-
Emission analyzer	NOx (ppm)	0–10000	20	2.80
	SOOT (mg/m^3)	0–50	0.001	0.30

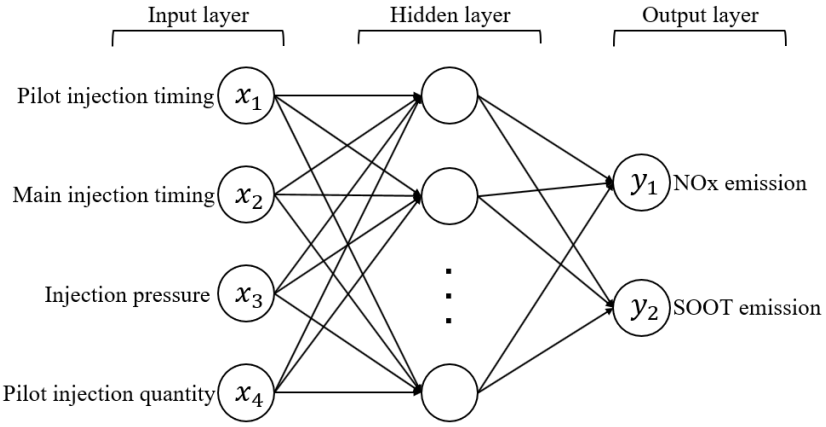

Fig. 2 Architecture of ANN

cooling water temperature, injection pressure, pilot and main injection timing, and pilot and main injection quantities. The experimental data in this study were obtained on a fixed engine bench, and the control factors other than the engine itself were considered fixed. A non-linear relationship exists between the injection parameters and emissions. Generally, with more training data in a prediction model, the accuracy is higher. However, more data requires more experiments, which leads to a significant increase in experimental cost. After comprehensive consideration, typical operating conditions with 112 trials were selected for the arrangement of the operating points. Table 3 lists the original injection parameters and single adjustment range of the engine at the usual speed and load. The variation of main injection quantity is automatically defined from the original MAP data of ECU when the four variables of pilot injection timing, main injection timing, injection pressure and pilot injection quantity are adjusted at the test operations. Based on these basic conditions, only one injection parameter was adjusted for each measurement. The accuracies and uncertainties of the measurement equipment are listed in Table 4.

2.2 Artificial Neural Network

ANN have found extensive application in information processing, pattern recognition, signal control, and system prediction, and have shown strong potential to solve highly complex non-linear problems. A three-layer feed-forward back propagation network, which is the most widely used neural network (Dhande et al., 2022; Fu et al., 2022; Sivamani et al., 2022) is developed in this study. The input and output layers are connected by a hidden layer using transfer functions, as shown in Fig. 2. The ANN model uses the sigmoid function as the activation function, with smooth, continuous properties. A backpropagation algorithm is selected to calculate the weight values of the network. As a single hidden layer can map all continuous functions (Poggio & Girosi, 1990), in

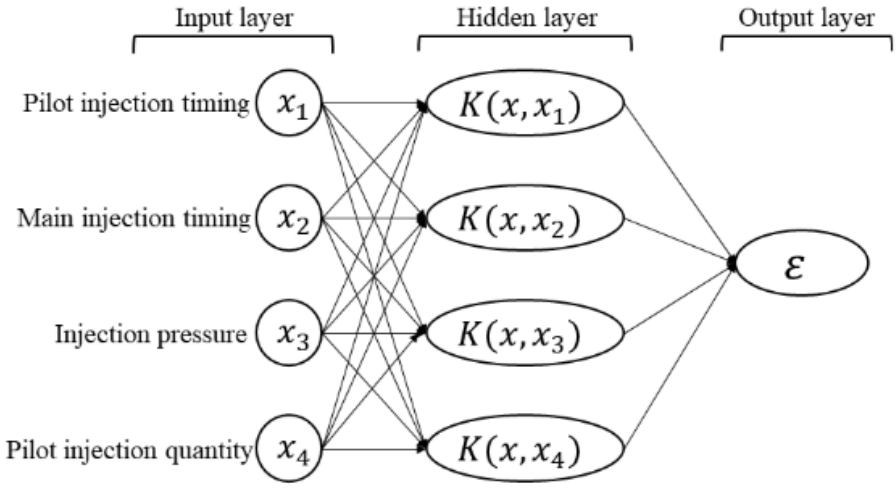

Fig. 3 Architecture of SVM

order to improve the efficiency of training and prediction, a single hidden layer structure is preferred in this study.

The function of the ANN for prediction can be expressed as

$$E = \frac{1}{2}\sum_{i=1}^{n}(y_i - z_i)^2 \tag{1}$$

where, n is the total number of samples; i is the *ith* sample, E is the output error; and y_i and z_i are the predicted and actual values of the output layer for the *ith* sample, respectively. The output layer was decreased over several iterations until the convergence condition was satisfied.

2.3 Support Vector Machine

The Support Vector Machine (SVM) was first developed by Vapnik (2000), and is a type of machine learning algorithm based on structural risk minimization derived from solving two types of pattern recognition problems. It is a type of data modeling approach that identifies appropriate kernel functions that implicitly map non-linear data to a high-dimensional space, thus converting the non-linear problem to a linear model that is easily solved. Common kernel functions include radial basis, polynomial, sigmoid, and linear kernel functions. In existing research and industry, the radial basis function has the widest range of applications and is used in this study. After determining the kernel function, the kernel function parameters must be set. Vapnik et al. showed that the penalty parameter and width coefficient are the main factors affecting the SVM performance. An SVM is employed in this study, which creates an optimal design between learning efficiency and prediction accuracy by extracting information from sample data. Similar to the ANN, the same samples were used to train the model, and the injection parameters were used as inputs. The architecture of the SVM is illustrated in Fig. 3.

Generally, a penalty function is adopted to transform a regression problem into a constrained optimization problem, which can be defined as

$$minQ(\omega, b, \xi, \xi^*) = \frac{1}{2}\omega^T\omega + C\sum_{i=1}^{l}(\xi_i + \xi_i^*) \tag{2}$$

$$\text{s.t.}\begin{cases} y_i - \omega\cdot\varphi(x_i) - b \le \varepsilon + \xi_i \\ \omega\cdot\varphi(x_i) + b - y_i \le \varepsilon + \xi_i^* \\ \xi_i \ge \xi_i^* \ge 0,\ i = 1,2,\ldots,l \end{cases} \tag{3}$$

where, ω is the weight matrix of different factors, b is the bias term, ε is the loss function, ξ and ξ^* represent relaxation variables, C is the penalty factor, and $\varphi: x \to f$ is a non-linear variable that changes the input space into a high-dimensional space.

By selecting the proper kernel function and Lagrange multiplier, the above constrained optimization problem is extended to a SVM regression problem, as shown in Eq. (4) (Kavitha & Mukesh Kumar, 2018).

$$f(x) = \sum_{i=1}^{l}(\alpha_i - \alpha_i^*)k(x_i, x) + b \tag{4}$$

where, k is the kernel function, and $(\alpha_i - \alpha_i^*)$ is the Lagrange multiplier.

3. RESULTS AND DISCUSSION

To ensure the accuracy of the model, 80 percent of the experimental points were randomly selected as training samples, and the remaining points were used as testing samples. Based on the training samples, the ANN and SVM were trained to predict SOOT and NOx emissions. The injection parameters, including the pilot injection timing, main injection timing, injection pressure, pilot injection quantity, and engine operating parameters, including speed and load, were chosen as inputs.

Order-of-magnitude differences among different influencing factors often lead to a reduction in the prediction accuracy and training speed of the model. To avoid masking of variables of a small order of magnitude by parameters of a large order of magnitude, the input parameters were normalized before training and the output parameters were anti-normalized after training. The normalization function is

$$\bar{x} = -1 + \frac{2(x - x_{\min})}{x_{\max} - x_{\min}} \tag{5}$$

where, x is the variable to be normalized, $x_{\min}$ is the minimum value of the variable, $x_{\max}$ is the maximum value of the variable, and $\bar{x}$ is the normalized variable.

Simultaneously, the predictive performances were evaluated using mean square error (MSE) and determination coefficient (R^2) (Niu et al., 2017), which are defined as

$$MSE = \frac{1}{n}\sum_{i=1}^{n}(\hat{y}_i - y_i)^2 \tag{6}$$

$$R^2 = \frac{\left(n\sum_{i=1}^{n}\hat{y}_i y_i - \sum_{i=1}^{n}\hat{y}_i \sum_{i=1}^{n} y_i\right)^2}{\left[n\sum_{i=1}^{n}\hat{y}_i^2 - \left(\sum_{i=1}^{n}\hat{y}_i\right)^2\right]\left[n\sum_{i=1}^{n} y_i{}^2 - \left(\sum_{i=1}^{n} y_i\right)^2\right]} \tag{7}$$

where, n is the total number of points, and $\hat{y}_i$ and y_i represent the *ith* target and predicted values, respectively.

3.1 Artificial Neural Network Evaluation

Considering that the predictive performance of an ANN is significantly affected by the network structure and learning rules, the selection and optimization of the training function, neurons, and iterations were analyzed by determining the MSE between the target and predicted values in this study. To ensure the rationality of the parameters, the training function and number of neurons in the ANN were changed successively. According to the empirical formula, the number of hidden-layer neurons ranged from 3 to 20. The maximum number of iterations was set as 1000 and the threshold to stop training was set as 10^{-5} in this study. The variation in the MSE with the number of hidden layer neurons under different training functions, such as trainlm, traingda, and trainrp, is shown in Figs. 4 and 5.

MSE was employed to describe the accuracy of the ANN, and lower numbers indicate better accuracy. In Fig. 4, with an increase in the number of neurons from 3 to 20, the MSE for SOOT fluctuates between 0.01 and 0.74. The MSE values of the three algorithms fluctuate, and the fluctuation trend is consistent, which indicates that the fluctuation of the MSE is related to the difference in the input data under the same algorithm. In contrast, the MSE of the trainlm algorithm is the smallest, and the minimum MSE is 0.011, when the number of neurons is 10. As shown in Fig. 5, with an increase in the number of neurons, the MSE for NOx fluctuates between 0.042 and 3. Apart from trainlm, the MSE of the other algorithms exhibit local fluctuations. When the number of neurons is between 10 and 14, the minimum MSE is achieved for all algorithms. With variation in the number of hidden layer neurons, the MSE of the trainlm algorithm is always at a minimum. When the number of neurons is 12, the minimum MSE is 0.042. Subsequently, the MSE slowly increases with an increase in the number of neurons. Considering the prediction accuracy and calculation time, the trainlm algorithm was selected for this study.

Figurs 6 and 7 compare the MSE of the ANN models

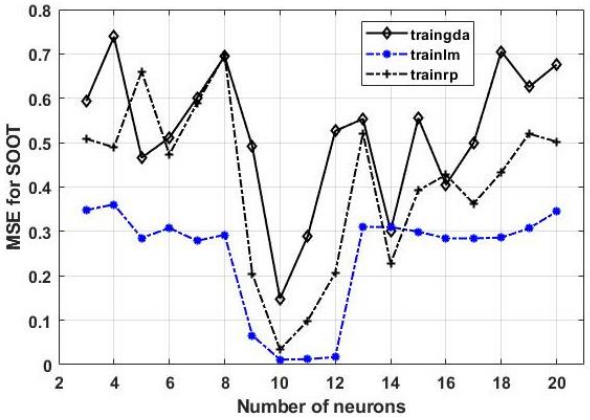

Fig. 4 The MSE for SOOT with variation of neurons under different training functions

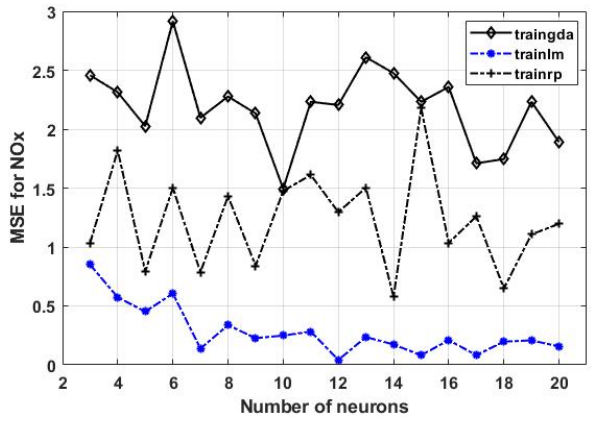

Fig. 5 The MSE for NOx with variation of neurons under different training functions

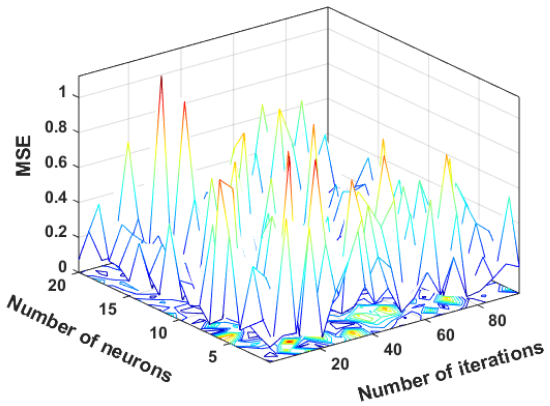

Fig. 6 MSE distribution with different ANN parameters for SOOT

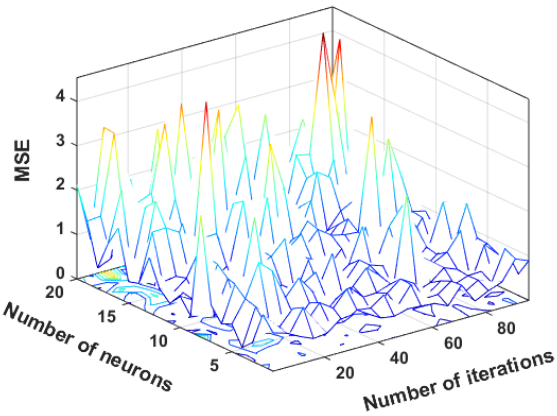

Fig. 7 MSE distribution with different ANN parameters for NOx

for SOOT and NOx emissions, respectively, which were investigated with different numbers of neurons and iterations.

The performance of the ANN was evaluated by comparing the MSE of the SOOT and NOx emissions with different model parameters, which were distinctly different from the changes in the predictors. As shown in Fig. 6, the MSE distribution with different ANN parameters for SOOT fluctuates within a certain range from 0 to 1, indicating that the accuracy of the ANN is unstable because of different numbers of iterations and neurons. In Fig. 7, the MSE distribution with different ANN parameters for NOx fluctuates over a wide range from 0 to 4, which is mainly due to the large magnitude of the NOx measurement data. In contrast, the MSE of NOx fluctuates gently, which means that the predicted value coincides well with the target value when the ANN is applied for NOx modeling. When the number of neurons is determined, the MSE of the test set fluctuates within a small range with variations in the network iterations, and the prediction performance of the neural network is more stable. A comparative analysis shows that the number of neurons has a greater effect than the number of network iterations. An ANN with too many or too few neurons can have a large MSE, and the best selection for neuron times can also vary. Too few neurons can lead to a low precision of ANN prediction and difficulty in handling complex nonlinear problems. When the number of neurons is excessive, the ANN is overtrained, and the training time is multiplied (Bittencout & Zárate, 2011). Accordingly, the appropriate parameters should be selected based on the research objectives.

Based on this inference, the number of neurons and iterations were selected based on the minimum MSE, as shown in Table 5. The results indicate that the ANN of SOOT emissions with 10 neurons in the hidden layers and 11 iterations has the minimum MSE. For comparison, the best NOx emission parameters were selected using 12 neurons and 33 iterations. The corresponding minimum MSE values are 0.011 and 0.042, respectively. The ANN model was established using the optimal hidden layer neurons and number of iterations.

3.2 Support Vector Machine Evaluation

Based on the training data, the relationship between the engine emissions and injection parameters was investigated using an SVM with Radial Basis Function (RBF) kernel. As described in the previous section, the penalty parameter (C) and width coefficient (g) of the RBF kernel significantly affects the SVM performance. However, there is no unified method for determining these

Table 5 Best parameters for the ANN Model

Parameter	SOOT	NOx
Training Function	trainlm	trainlm
Neurons	10	12
Iterations	11	33
MSE	0.011	0.042

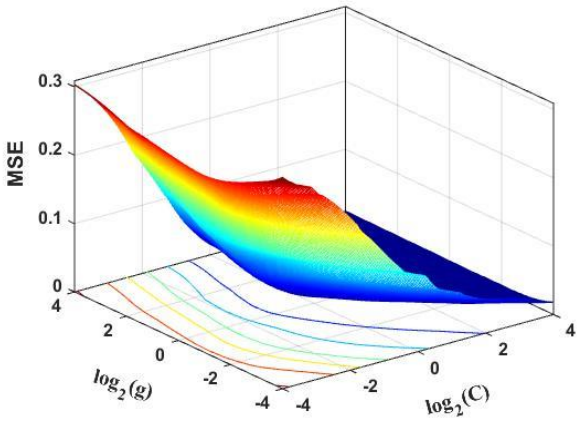

Fig. 8 MSE distribution with different SVM parameters for SOOT

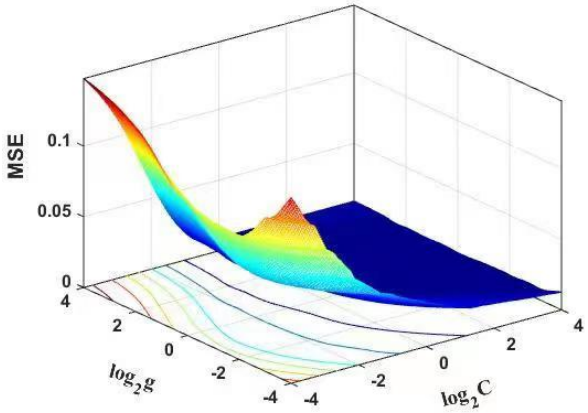

Fig. 9 MSE distribution with different SVM parameters for NOx

parameters. In this study, a 5-fold cross-validation method was applied to optimize the SVM penalty and kernel parameters. Considering the computing efficiency and precision, the range of parameters was 2^{-4} – 2^{4} and the threshold to stop the training was set as 10^{-7}. The MSE of the SVM model based on different C and g are compared in Figs. 8 and 9.

It can be concluded from Figs. 8 and 9 that the MSE values of the SVM for NOx and SOOT show different change rules with different parameters. The choice of appropriate parameters enables the model to have excellent capabilities, which provide a basis for the selection of parameters. The effect of C on the prediction accuracy of the SVM follows certain laws. Generally, with an increase in C, the degree of data fitting is higher, but the generalization ability is worse. Considering the SVM for SOOT as an example, with the enhancement of the penalty parameter, the MSE of the SVM decreases sharply, while it remains at 0.05 when the penalty parameter is greater than one. The same variation is observed for NOx. The influence of g on the MSE of the SVM is not significant when C is a fixed value, whereas the model performance significantly improves with change in C in a certain range when g is a fixed value. Thus, the effect of g on improving the performance of the

Table 6 Best parameters for the SVM Model

Parameter	SOOT	NOx
$\log_2(C)$	3.981	3.203
$\log_2(g)$	-1.012	-3.955
MSE	0.053	0.014

SVM is weaker than that of *C*, which is also evident in the contour lines in the figures. However, the training samples are overfitted or underfitted, when g continues to increase or decrease.

The two parameters have certain efficiency and application boundaries, and parameter selection should be considered when determining the research objects. The optimal parameters for the SVM with the minimum MSE are listed in Table 6. As shown in Table 6, the minimum MSE values obtained for SOOT and NOx are 0.053 and 0.014, respectively, indicating that the SVM models for different engine emissions are trained well. In addition, $\log_2(C)$ is 3.981 and 3.203, while $\log_2(g)$ is -1.012 and -3.955 for SOOT and NOx, respectively, when the MSE is minimal. Finally, the parameter combination with the minimum MSE is selected as the optimal combination.

3.3 Comparison of Generalization Ability Between ANN and SVM

As typical intelligent machine-learning algorithms, ANN and SVM summarize the inner laws of the input patterns from limited samples through training and learning. The trained models can predict outputs with high precision. The generalization ability of a model reflects its ability to predict new data. In general, the tested determination coefficient (R^2) is selected to evaluate the generalization ability.

To better utilize the sample information, the R^2 values of the training and test data were compared as shown in Figs. 10-13. For different emissions, there are certain differences in the generalization abilities of the ANN and SVM. The R^2 values of the training and test data deviate significantly from the fitted straight line and are relatively dispersed in Figs. 10 and 11. Thus, the generalization

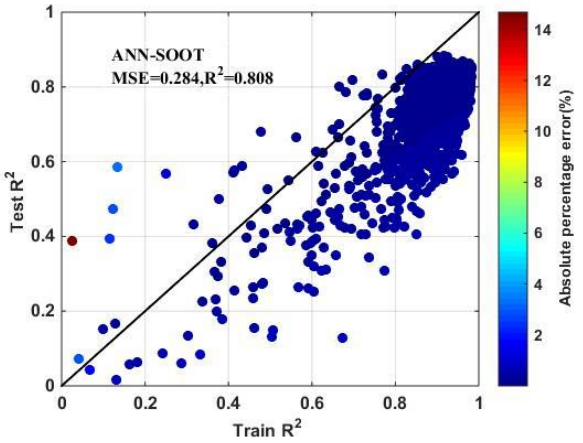

Fig. 10 Determination coefficient of ANN for SOOT

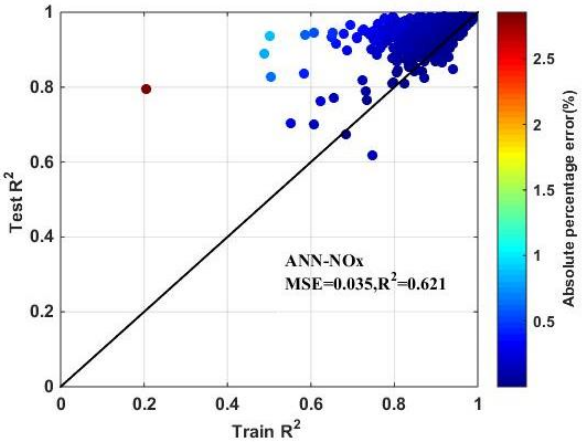

Fig. 11 Determination coefficient of ANN for NOx

ability of the ANN is poor. In addition, the R^2 value of the test data does not increase with the R^2 value of the training data, as shown in Figs. 10 and 11, and there is no fixed change rule. The generalization ability of the ANN exhibits some randomness and uncertainty. The R^2 values of the ANN for SOOT and NOx emissions are 0.808 and 0.621, respectively. The R^2 value of the training set is generally smaller than that of the test set, as shown in Fig. 10, indicating that the training samples overfits in the ANN model. Overfitting occurs when the number of samples is too less, and the training of ANNs generally requires a large number of samples.

In Figs. 12 and 13, the R^2 values of the training and test data exhibit the same variation trend. The performance of the training set reflects the predictive performance of the SVM model on the test set, indicating that the SVM has good generalization ability. The data points in Fig. 13 are distributed more evenly on the left and right sides of the diagonal. The R^2 values of the training and test data for NOx are closer to the fitting line than those for SOOT, which shows that the input and output variables of the sample data have a certain influence on the generalization ability of the SVM. This is because the soot generation process is complex and the data fluctuates significantly. The R^2 values of the SVM for SOOT and NOx are 0.825 and 0.914, respectively. The comparison between R^2 indicates that the SVM has better generalization ability

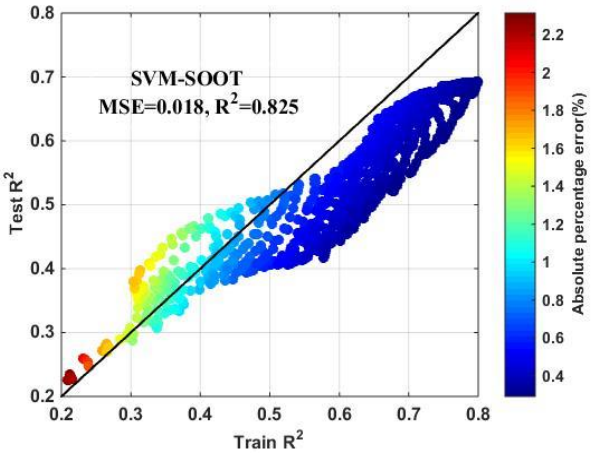

Fig. 12 Determination coefficient of SVM for SOOT

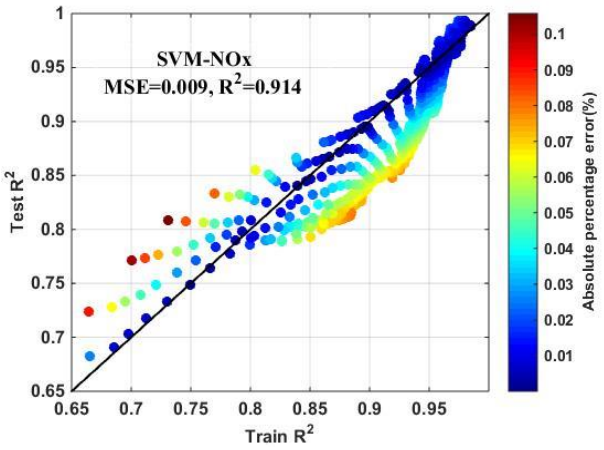

Fig. 13 Determination coefficient of SVM for NOx

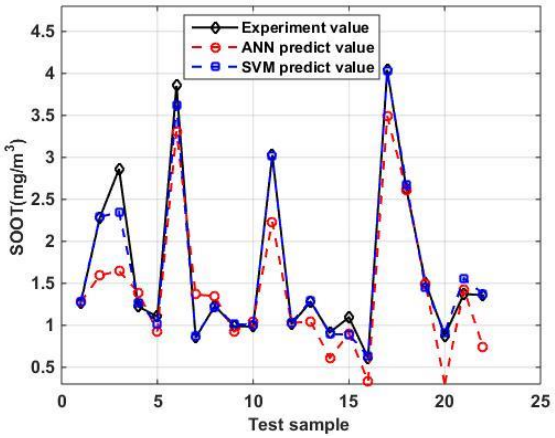

Fig. 14 The prediction results of ANN and SVM for SOOT

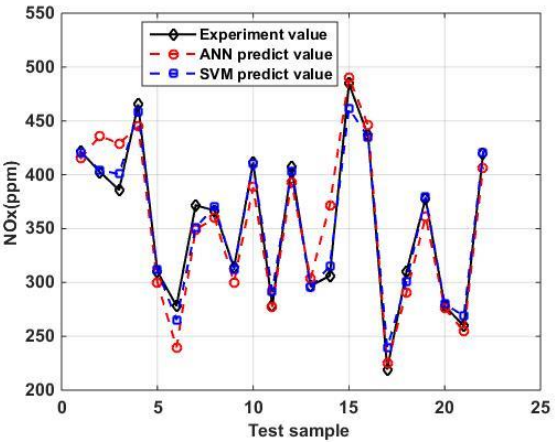

Fig. 15 The prediction results of ANN and SVM for NOx

than the ANN in engine emission prediction. From a local perspective, when the training R^2 increases, the test R^2 exhibits a certain degree of decline. This indicates that the complexity of SVM increases when the number of misclassified samples is reduced during the training process of the prediction model. In the actual problem-solving process, the parameters can be optimized and trained effectively. Hence, an SVM prediction model with excellent performance is established to improve the generalization ability.

Moreover, the MSE values of the SVM for SOOT and NOx are 0.018 and 0.009, respectively, which are smaller than the values of 0.284 and 0.035 predicted by the ANN. It can be concluded that the dispersion is improved using the SVM, which also suggests that the SVM has good generalization ability depending on the selection of proper model parameters.

3.4 Comparison of Prediction Accuracy Between ANN and SVM

To compare the prediction accuracy of the ANN and SVM for the engine emission response, Figs. 14 and 15 show the prediction results of the ANN and SVM. It is clear that both have excellent degree of fitting between the predicted and test values for the engine response. The prediction results of the SVM are better than those of the ANN. Comparing the relative error of the 22 test samples, the maximum error of the SVM is less than 10%, whereas the maximum error of the ANN is more than 30%. The prediction error of the ANN model is relatively large under certain working conditions, and even shows the opposite trend. This is because the ANN minimizes the MSE through continuous backpropagation learning, whereas the SVM adjusts the parameters of the kernel function for training samples through cross-validation and aims to minimize the structural risk. The predicted values of the SVM for the test samples are also very close to the experimental values in the figures, indicating that the performance of the SVM prediction model is relatively stable, and the prediction accuracy is higher.

The MSE and R^2 values of test samples are listed in Table 7 for comparison. For SOOT and NOx, the R^2 values of the SVM are close to 1 (0.983 and 0.982, respectively), whereas those for the ANN are 0.934 and 0.885,

Table 7 The MSE and R^2 values of test samples

Test	MSE	R^2
SVM for SOOT	0.019	0.983
SVM for NOx	103.465	0.982
ANN for SOOT	0.035	0.934
ANN for NOx	164.570	0.885

respectively. The MSE values of the SVM for SOOT and NOx are also smaller than those of the ANN, which are 0.019 and 103.465, respectively. All comparisons demonstrate that the SVM model performs better than the ANN model in predicting engine emissions. From the results, it is evident that the SVM can optimize the model parameters by using the cross-validation method and has good predictive accuracy. However, an ANN parameter optimization method should be developed and designed to improve its performance.

3.5 Optimization of Injection Parameters to Improve the SOOT/NOx Trade-Off

A trade-off exists between SOOT and NOx emissions, which are the main emissions of diesel engines. To reduce diesel engine emissions, SOOT and NOx emissions must

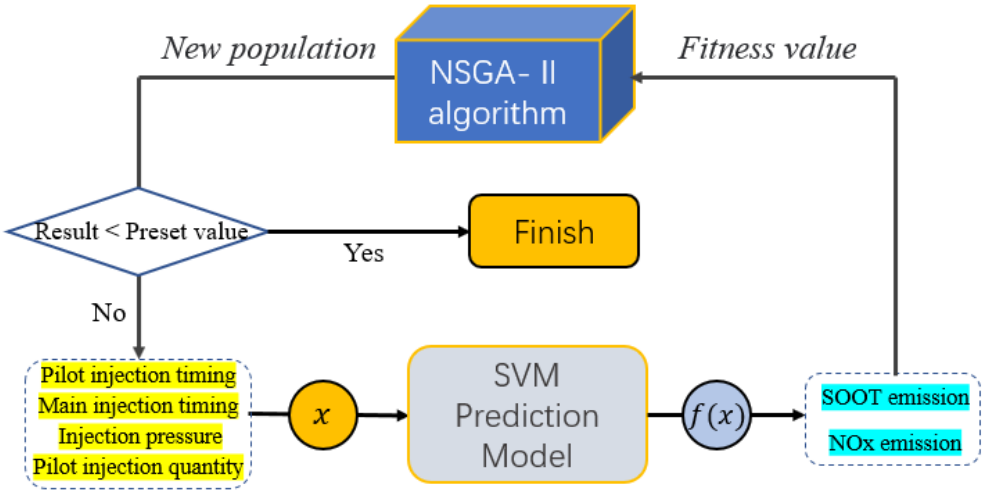

Fig. 16 Optimization process

be considered. This is a multi-objective optimization problem, and the aim is to achieve the optimal value of multiple sub-objectives. SOOT emissions were selected as Target 1 and NOx emissions as Target 2. In general, it can be transformed into an extreme value for multiple objective functions under certain constraints. The emission indicators CO and HC were restricted according to the requirements of the emission regulations, and the mathematical model was established as follows:

$$min\, f_1(x) = SOOT(x) \tag{8}$$

$$min\, f_2(x) = NO_x(x) \tag{9}$$

$$s.t. \begin{cases} g_1(x) = HC(x) \le 0.9T_{HC} \\ g_2(x) = CO(x) \le 0.9T_{CO} \end{cases} \tag{10}$$

$$x \in (x_1, x_2, x_3, x_4) \tag{11}$$

where, x is the decision variable that includes the pilot injection timing, main injection timing, injection pressure, and pilot injection quantity; T_{HC} and T_{CO} are the emission regulatory standard limit, the safety coefficient is 0.9, and $g_1(x)$ and $g_2(x)$ are the constraint functions.

The SVM model established in this study is stable and reliable in predicting engine emissions, and has obvious advantages compared with the ANN model. Based on the optimal SVM model developed in Section 3.2, the non-dominated sorting genetic algorithm-II (NSGA-II) (Huang et al., 2022) was used to determine the optimal solution set of the injection parameters under the corresponding engine operating conditions, which is the basis for optimizing the injection parameters of the F-T diesel engine. Figure 16 shows the specific optimization process.

First, the NSGA-II algorithm fixes the speed and torque of the corresponding operating conditions, and randomly generates four injection parameters populations that are used as the input of the SVM model. The corresponding output value of each population is then calculated using the SVM model and input into the NSGA-II algorithm as the fitness value. Finally, NSGA-II evaluates the better individuals in the current population and repeats the process until the maximum evolutionary algebra of NSGA-II is reached. Considering the accuracy of the optimal solution and computational efficiency, the population size was 30 and the maximum evolutionary algebra was 80.

Figure 17 shows the optimized populations for the SOOT and NOx emissions. In Fig. 17, the pentagram symbols represent the SOOT and NOx emissions of the original diesel engine under the four operating conditions. The circular symbols represent the original populations and octagonal symbols represent the optimized solutions for SOOT and NOx emissions. It is evident that NOx emissions decrease and SOOT emissions increase at the same time, which indicates a clear trade-off relationship. Thirty individuals were in the leading position under the four operating conditions, indicating that optimization was completed. The SOOT and NOx emissions decrease simultaneously in the optimized solutions under all operating conditions, which can provide optional injection parameters for the engine. Compared with the original engine operating conditions, the SOOT emissions of the optimized solutions decrease by 3.7–7.1%, and the NOx emissions decrease by 1.2–2.6% on average. Refer to the original ratio of SOOT and NOx emissions， optimal injection parameters combination under different operating condition are listed in Table 8.

4. CONCLUSIONS

This study aims to predict engine performance using non-linear modeling and finding the optimal model parameters as a reference to improve the SOOT-NOx trade-off. ANN and SVM models based on engine sample models were applied to predict the emissions, and the models were compared with the same training data. The main conclusions are as follows.

(1) The ANN and SVM models based on the optimal parameters show excellent accuracy and stability in addressing non-linear systems, indicating that the characteristics of the training samples can be obtained automatically by the ANN and SVM. The output can be accurately forecast based on the input sample.

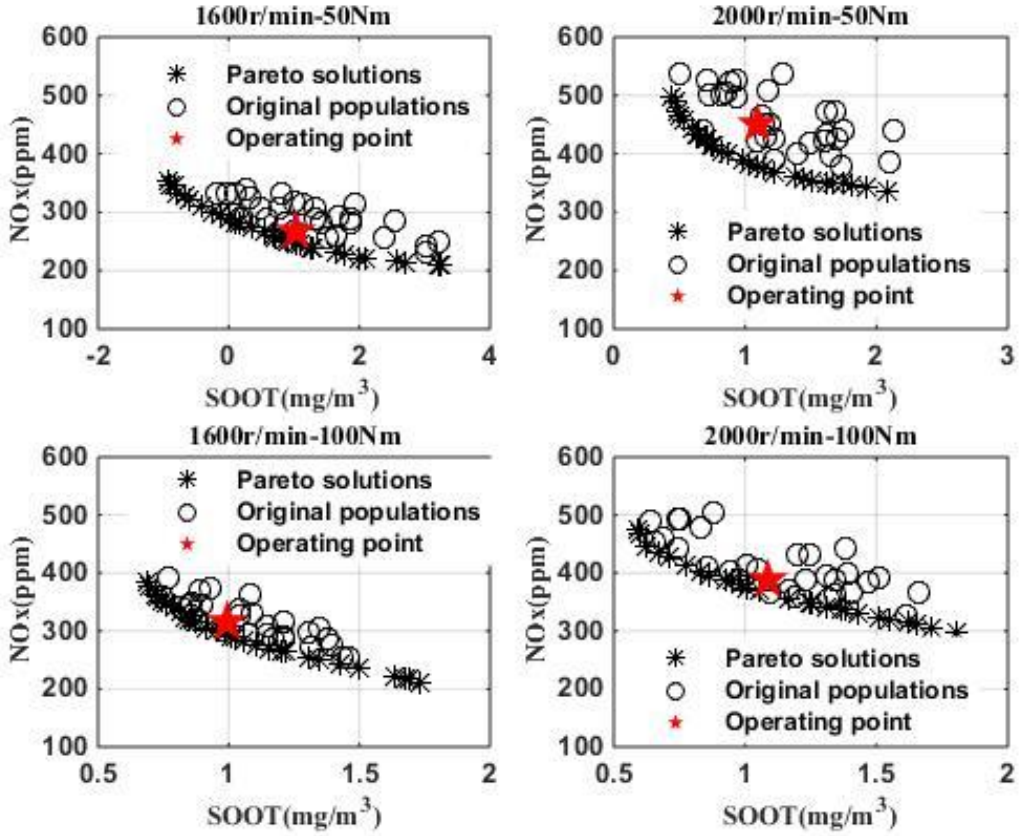

Fig. 17 The Pareto solutions for SOOT and NOx emissions

Table 8 Optimal injection parameters combination under different operating condition

Speed(r/min) -Torque (Nm)		Pilot injection timing (°CA BTDC)	Main injection timing (°CA BTDC)	Injection pressure (MPa)	Pilot injection quantity (mg/cyc)	SOOT Emission (mg/m^3)	NOx Emission (ppm)
1600 -50	Operation point	11.4	4.6	69.0	1.86	3.04	268
	Optimized parameter	8.5	3.2	74.6	1.89	2.89	250
1600 -50	Operation point	13.5	5.4	88.1	2.05	1.09	452
	Optimized parameter	9.1	3.7	92.9	1.82	1.03	381
2000 -50	Operation point	12.0	5.2	77.0	1.88	0.99	314
	Optimized parameter	10.9	4.1	84.5	1.71	0.98	296
2000 -100	Operation point	14.0	5.9	95.0	2.08	1.09	389
	Optimized parameter	11.8	4.5	102.3	1.51	1.05	370

(2) The comparison of ANN and SVM suggests that SVM has a higher predictive accuracy and generalization ability, whereas ANN may lead to overfitting. SVM is a promising approach for engine emission prediction. Some defects, such as slow convergence speed and large MSE can be improved by optimizing the kernel function and penalty factor through cross-validation.

(3) The optimal SVM model was combined with the NSGA-II algorithm to decrease NOx and SOOT emissions and obtain the corresponding optimal Pareto solution set. This provides a basis for optimizing the diesel injection parameters to improve the SOOT-NOx trade-off.

ACKNOWLEDGEMENTS

The authors would like to acknowledge the financial support by the National Natural Science Foundation of China (Grant No. 51805353) and the research project was supported by Shanxi Scholarship Council of China (Grant No. HGKY2019041).

CONFLICT OF INTEREST

No conflict of interest exists in this article and the authors have no conflicts to disclose.

AUTHORS CONTRIBUTION

Conceived and designed the article: J. H. Shi, W. R. Liao. Performed the experiments: J. H. Shi. Analyzed the data: W. R. Liao. Contributed materials: G. X. Li. Wrote the paper: W. R. Liao, J. H. Shi.

REFERENCES

Aydın, M., Uslu, S., & Bahattin Çelik, M. (2020). Performance and emission prediction of a compression ignition engine fueled with biodiesel-diesel blends: A combined application of ANN and RSM based optimization. *Fuel*, 269, 117472. https://doi.org/https://doi.org/10.1016/j.fuel.2020.117472

Bittencout, F. R., & Zárate, L. E. (2011). Hybrid structure based on previous knowledge and GA to search the ideal neurons quantity for the hidden layer of MLP—Application in the cold rolling process. *Applied Soft Computing*, 11(2), 2460-2471. https://doi.org/https://doi.org/10.1016/j.asoc.2010.10.002

Chandran, D. (2020). Compatibility of diesel engine materials with biodiesel fuel. *Renewable Energy*, 147, 89-99. https://doi.org/https://doi.org/10.1016/j.renene.2019.08.040

Dhande, D. Y., Choudhari, C. S., Gaikwad, D. P., & Dahe, K. B. (2022). Development of artificial neural network to predict the performance of spark ignition engine fuelled with waste pomegranate ethanol blends. *Information Processing in Agriculture*. https://doi.org/https://doi.org/10.1016/j.inpa.2022.05.001

Duan, H., Huang, Y., Mehra, R. K., Song, P., & Ma, F. (2018). Study on influencing factors of prediction accuracy of support vector machine (SVM) model for NOx emission of a hydrogen enriched compressed natural gas engine. *Fuel*, 234, 954-964. https://doi.org/https://doi.org/10.1016/j.fuel.2018.07.009

Emiroğlu, A. O., & Şen, M. (2018). Combustion, performance and exhaust emission characterizations of a diesel engine operating with a ternary blend (alcohol-biodiesel-diesel fuel). *Applied Thermal Engineering*, 133, 371-380. https://doi.org/https://doi.org/10.1016/j.applthermaleng.2018.01.069

Fu, J., Yang, R., Li, X., Sun, X., Li, Y., Liu, Z., Zhang, Y., & Sunden, B. (2022). Application of artificial neural network to forecast engine performance and emissions of a spark ignition engine. *Applied Thermal Engineering*, 201, 117749. https://doi.org/https://doi.org/10.1016/j.applthermaleng.2021.117749

Guardiola, C., López, J. J., Martín, J., & García-Sarmiento, D. (2011). Semiempirical in-cylinder pressure based model for NOX prediction oriented to control applications. *Applied Thermal Engineering*, 31(16), 3275-3286. https://doi.org/https://doi.org/10.1016/j.applthermaleng.2011.05.048

Gürgen, S., Ünver, B., & Altın, İ. (2018). Prediction of cyclic variability in a diesel engine fueled with n-butanol and diesel fuel blends using artificial neural network. *Renewable Energy*, 117, 538-544. https://doi.org/https://doi.org/10.1016/j.renene.2017.10.101

Hao, B., Song, C., Lv, G., Li, B., Liu, X., Wang, K., & Liu, Y. (2014). Evaluation of the reduction in carbonyl emissions from a diesel engine using Fischer–Tropsch fuel synthesized from coal. *Fuel*, 133, 115-122. https://doi.org/https://doi.org/10.1016/j.fuel.2014.05.025

Hao, D., Mehra, R. K., Luo, S., Nie, Z., Ren, X., & Fanhua, M. (2020). Experimental study of hydrogen enriched compressed natural gas (HCNG) engine and application of support vector machine (SVM) on prediction of engine performance at specific condition. *International Journal of Hydrogen Energy*, 45(8), 5309-5325. https://doi.org/https://doi.org/10.1016/j.ijhydene.2019.04.039

Huang, Z., Huang, J., Luo, J., Hu, D., & Yin, Z. (2022). Performance enhancement and emission reduction of a diesel engine fueled with different biodiesel-diesel blending fuel based on the multi-parameter optimization theory. *Fuel*, 314, 122753. https://doi.org/https://doi.org/10.1016/j.fuel.2021.122753

Jiao, Y., Liu, R., Zhang, Z., Yang, C., Zhou, G., Dong, S., & Liu, W. (2019). Comparison of combustion and emission characteristics of a diesel engine fueled with diesel and methanol-Fischer-Tropsch diesel-biodiesel-diesel blends at various altitudes. *Fuel*, 243, 52-59. https://doi.org/https://doi.org/10.1016/j.fuel.2019.01.107

Kavitha, R., & Mukesh Kumar, P. C. (2018). A Comparison between MLP and SVR Models in Prediction of Thermal Properties of Nano Fluids. *Journal of Applied Fluid Mechanics*, 11, 7-14. https://doi.org/10.36884/jafm.11.SI.29411

Kim, Y. D., Yang, C. W., Kim, B. J., Moon, J. H., Jeong, J. Y., Jeong, S. H., Lee, S. H., Kim, J. H., Seo, M. W., Lee, S. B., Kim, J. K., & Lee, U. D. (2016). Fischer–tropsch diesel production and evaluation as alternative automotive fuel in pilot-scale integrated biomass-to-liquid process. *Applied Energy*, 180, 301-312. https://doi.org/https://doi.org/10.1016/j.apenergy.2016.07.095

Krishnamoorthi, M., Malayalamurthi, R., & Sakthivel, R. (2019). Optimization of compression ignition engine fueled with diesel - chaulmoogra oil - diethyl ether blend with engine parameters and exhaust gas recirculation. *Renewable Energy*, 134, 579-602. https://doi.org/https://doi.org/10.1016/j.renene.2018.11.062

Meenal, R., & Selvakumar, A. I. (2018). Assessment of SVM, empirical and ANN based solar radiation prediction models with most influencing input parameters. *Renewable Energy*, 121, 324-343. https://doi.org/https://doi.org/10.1016/j.renene.2017.12.005

Molina, S., Guardiola, C., Martín, J., & García-Sarmiento, D. (2014). Development of a control-oriented model to optimise fuel consumption and NOX emissions in a DI Diesel engine. *Applied Energy*, 119, 405-416. https://doi.org/https://doi.org/10.1016/j.apenergy.2014.01.021

Neves, R. C., Klein, B. C., da Silva, R. J., Rezende, M. C. A. F., Funke, A., Olivarez-Gómez, E., Bonomi, A., & Maciel-Filho, R. (2020). A vision on biomass-to-liquids (BTL) thermochemical routes in integrated sugarcane biorefineries for biojet fuel production. *Renewable and Sustainable Energy Reviews*, 119, 109607. https://doi.org/https://doi.org/10.1016/j.rser.2019.109607

Niu, X., Yang, C., Wang, H., & Wang, Y. (2017). Investigation of ANN and SVM based on limited samples for performance and emissions prediction of a CRDI-assisted marine diesel engine. *Applied Thermal Engineering*, 111, 1353-1364. https://doi.org/https://doi.org/10.1016/j.applthermaleng.2016.10.042

Pastor, J. V., García, A., Micó, C., & Lewiski, F. (2020). An optical investigation of Fischer-Tropsch diesel and Oxymethylene dimethyl ether impact on combustion process for CI engines. *Applied Energy*, 260, 114238. https://doi.org/https://doi.org/10.1016/j.apenergy.2019.114238

Poggio, T., & Girosi, F. (1990). Regularization algorithms for learning that are equivalent to multilayer networks. *Science*, 247(4945), 978-982.

Şener, R. (2022). Numerical Investigation of Ducted Fuel Injection Strategy for Soot Reduction in Compression Ignition Engine. *Journal of Applied Fluid Mechanics*, 15(2), 475-489. https://doi.org/10.47176/jafm.15.02.33088

Shamshirband, S., Tabatabaei, M., Aghbashlo, M., Yee, P. L., & Petković, D. (2016). Support vector machine-based exergetic modelling of a DI diesel engine running on biodiesel–diesel blends containing expanded polystyrene. *Applied Thermal Engineering*, 94, 727-747. https://doi.org/https://doi.org/10.1016/j.applthermaleng.2015.10.140

Shi, J., Wang, T., Zhao, Z., Wu, Z., & Zhang, Z. (2019). Cycle-to-Cycle Variation of a Diesel Engine Fueled with Fischer–Tropsch Fuel Synthesized from Coal. *Applied Sciences*, 9(10), 2032. https://www.mdpi.com/2076-3417/9/10/2032

Shi, J., Wang, T., Zhao, Z., Yang, T., & Zhang, Z. (2018). Experimental Study of Injection Parameters on the Performance of a Diesel Engine with Fischer–Tropsch Fuel Synthesized from Coal. *Energies*, 11(12), 3280-3292. https://www.mdpi.com/1996-1073/11/12/3280

Sivamani, S., Udayakumar, M., & Sellappan, N. (2022). Prediction of single cylinder direct injection diesel engine performance fuelled with lemon peel oil biodiesel using artificial neural network. *Materials Today: Proceedings*. https://doi.org/https://doi.org/10.1016/j.matpr.2022.10.197

Soloiu, V., Wiley, J. T., Gaubert, R., Mothershed, D., Carapia, C., Smith, R. C., Williams, J., Ilie, M., & Rahman, M. (2020). Fischer-Tropsch coal-to-liquid fuel negative temperature coefficient region (NTC) and low-temperature heat release (LTHR) in a constant volume combustion chamber (CVCC). *Energy*, 198, 117288. https://doi.org/https://doi.org/10.1016/j.energy.2020.117288

Vapnik, V. N. (2000). *The Nature of Statistical Learning Theory*. The Nature of Statistical Learning Theory. https://doi.org/https://doi.org/10.1007/978-1-4757-3264-1_1

Vishwanathan, G., & Reitz, R. D. (2015). Application of a semi-detailed soot modeling approach for conventional and low temperature diesel combustion – Part I: Model performance. *Fuel*, 139, 757-770. https://doi.org/https://doi.org/10.1016/j.fuel.2014.08.026

Zhao, F., Yang, W., Zhou, D., Yu, W., Li, J., & Tay, K. L. (2017). Numerical modelling of soot formation and oxidation using phenomenological soot modelling approach in a dual-fueled compression ignition engine. *Fuel*, 188, 382-389. https://doi.org/https://doi.org/10.1016/j.fuel.2016.10.054